Langmuir

ARTICLE

pubs.acs.org/Langmuir

Structure and Thermodynamics of Lipid Bilayers on Polyethylene Glycol Cushions: Fact and Fiction of PEG Cushioned Membranes

Erik B. Watkins,[†] Rita J. El-khouri,[‡] Chad E. Miller,[⊥] Brian G. Seaby,[§] Jaroslaw Majewski,[¶] Carlos M. Marques,[#] and Tonya L. Kuhl[*,§,∥]

[†]Biophysics Graduate Group, [‡]Department of Chemistry, [§]Department of Chemical Engineering and Materials Science, and [∥]Department of Biomedical Engineering, University of California, Davis, California 95616, United States

[⊥]Stanford Synchrotron Radiation Lightsource, Menlo Park, California 94025, United States

[#]Institut Charles Sadron, Université de Strasbourg, CNRS-UPR 22, Strasbourg, 67034, France

[¶]Manuel Lujan Jr. Neutron Scattering Center, Los Alamos National Laboratory, Los Alamos, New Mexico 87545, United States

ABSTRACT: In developing well hydrated polymer cushioned membranes, structural studies are often neglected. In this work, neutron and X-ray reflectivity studies reveal that hybrid bilayer/polyethylene glycol (PEG) systems created from mixtures of phospholipids and PEG conjugated lipopolymers do not yield a hydrated cushion beneath the bilayer unless the terminal ends of the lipopolymers are functionalized with reactive end groups and can covalently bind (tether) to the underlying support surface. While reactive PEG tethered systems yielded bilayers with near complete surface coverage, a bimodal distribution of heights with sub-micrometer lateral dimensions was observed consisting of cushioned membrane domains and uncushioned regions in close proximity to the support. The membrane fraction cushioned by the hydrated polymer could be controlled by adjusting the molar ratio of lipopolymer in the bilayer. A general phase diagram based on the free energy of the various configurations is derived that qualitatively predicts the observed behavior and the resulting structure of such systems a priori. As further evidenced by ellipsometry, atomic force and fluorescence microscopy, the tethered system provides a simple means for fabricating small cushioned domains within a membrane.

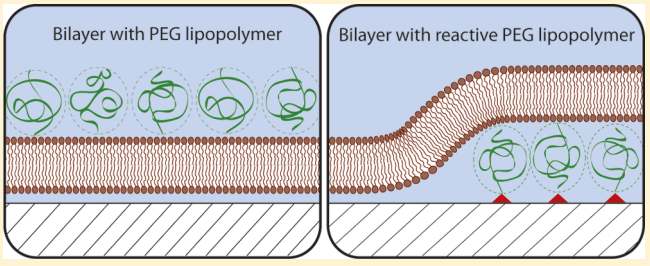

INTRODUCTION

A long-term goal for biophysical studies of membranes, transmembrane proteins, and lipid−protein interactions has been to fabricate biomimetic membranes on solid supports. However, the proximity of the solid substrate results in detrimental interactions between the substrate and protein frequently leading to protein denaturing or limited protein mobility.[1−3] The extent to which lipid packing and membrane organization is altered by interactions with the support also remains unclear. A highly hydrated "cushion" between the membrane and the underlying solid support may alleviate these effects and allow structural characterization of the membrane free from substrate interactions; their study under more biologically relevant conditions, and, in many cases, is a necessary prerequisite for the study of membrane proteins. To achieve this goal, a large research effort has been directed toward engineering polymeric cushions with beneficial properties.[1−9] However, structural characterization of cushioned membrane systems has been limited. This lack of information can potentially lead to misinterpretation of experimental data such as lipid and protein diffusion coefficients.

Due to its nonionic nature and biocompatibility, polyethylene glycol (PEG) has become a commonly used platform for cushioning membranes.[7,10−13] In this work, we investigated the structure of membranes supported by PEG lipopolymers. Two types of cushions were constructed: one with a reactive silane at the terminal end of the PEG to tether the lipopolymer to the underlying surface (DSPE-esPEG2k), similar to the system described by Tamm and co-workers, and the other lacking this reactive functionality (DSPE-PEG2k).[8] Typically, fluorescent microscopy is used to characterize the homogeneity and fluidity of such hybrid systems. For example, membranes containing such lipopolymers can routinely be deposited to yield a uniform fluorescent field as shown in Figure 1. Indeed, many studies in the literature have used fluorescent microscopy to suggest incorporation of lipopolymers yields homogenously cushioned membranes.[7,10−13] However, these results can be misleading and there has been little effort devoted to precise structural characterization of PEG membrane cushions. In this work, we use neutron and X-ray reflectometry as well as complementary techniques to investigate the structure and properties of several PEG membrane cushion preparations. We also provide a qualitative phase diagram that can be used to predict the resulting structure of such systems a priori.

Received: February 16, 2011
Revised: July 5, 2011
Published: July 05, 2011

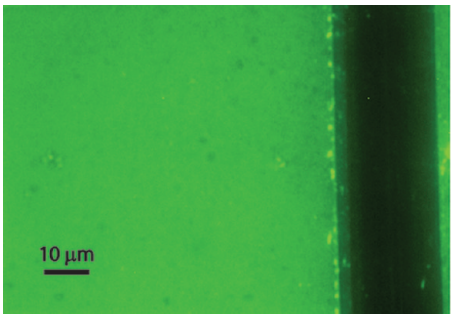

Figure 1. Fluorescent microscopy image of a DSPE-esPEG2k bilayer composed of 5 mol % lipopolymer and 2 mol % NBD-DPPE. The uniform field suggests the existence of a full coverage membrane without phase separation or lateral heterogeneities. The vertical dark line corresponds to a membrane region removed via scratching with tweezers.

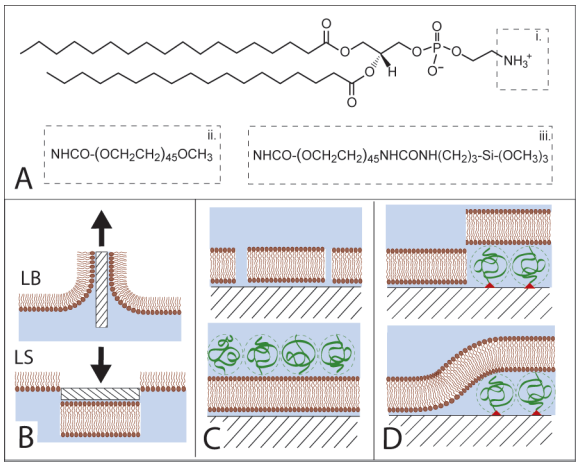

Figure 2

MATERIALS AND METHODS

Materials and Synthesis. Figure 2A shows the chemical structure of the lipids primarily used in this work. All lipids were purchased from Avanti Polar Lipids (Alabaster, AL): 1,2-distearoyl-*sn*-glycero-3-phosphoethanolamine (DSPE), 1,2-distearoyl-*sn*-glycero-3-phosphoethanolamine-*N*-[polyethylene glycol-2000] (DSPE-PEG2k), 1,2-distearoyl-*sn*-glycero-3-phosphoethanolamine-*N*-[amino(polyethylene glycol)2000] (amine terminated DSPE-PEG2k), 1,2-dipalmitoyl-*sn*-glycero-3-phosphocholine (DPPC), and 1-palmitoyl-2-oleoyl-*sn*-glycero-3-phosphocholine (POPC). Single crystal quartz substrates with ~3 Å rms roughness were obtained from Mark Optics (Santa Ana, CA) for X-ray reflectivity experiments and Institute of Electronic Materials and Technology (Warsaw, Poland) for neutron reflectivity experiments. Prior to use, the quartz substrates were sonicated in chloroform and Hellmanex soap solution, rinsed in Millipore-deionized water, and then dried under a stream of pure nitrogen (N_2). The substrates were then placed in a UV-ozone chamber for 30−40 min. The cleaned substrates were water wetting, with a contact angle of <10° as characterized via contact angle measurements.

An ethoxy silane terminated DSPE-PEG2k molecule (DSPE-esPEG2k) was synthesized from amine terminated DSPE-PEG2k and 3-(triethoxysilyl)propyl isocyanate obtained from Sigma-Aldrich. These two components were mixed in a 1:1 ratio and the reaction was conducted in chloroform and stirred for at least 24 h. Fourier transform infrared (FTIR) spectroscopy was used to measure loss of isocyanate functionality, and >98% conversion to the lipopolymer silane was obtained.

Sample Preparation. Bilayers were primarily prepared using the Langmuir−Blodgett/Langmuir−Schaeffer (LB/S) deposition technique. Lipids were dissolved at ~1.0 mg/mL in a 90:10 volume ratio chloroform and methanol mixture. For untethered PEG cushions, a 95:5 mol ratio of DSPE to DSPE-PEG2k was prepared and tethered PEG cushions were prepared from 98:2, 95:5, 93.5:6.5, and 90:10 mol ratio DSPE/DSPE-esPEG2k mixtures. Spreading solutions were deposited onto an ultrapure water subphase, and solvent was allowed to evaporate. Monolayers were compressed to yield tightly packed lipid films (40−45 mN/m) and allowed to equilibrate for at least 15 min before depositing. For DSPE-esPEG2k mixtures, the subphase was adjusted to pH ~ 4 through the addition of HCl. Acidic conditions aid hydrolysis of the ethoxy groups, allowing polycondensation, and promote silane binding to hydroxyl groups on the quartz surface. For DSPE and DSPE-PEG2k mixtures, a 5−10 mm/min dip speed was typically used for depositing the inner leaflet on 75 mm diameter quartz substrates. For DSPE-esPEG2k mixtures, a slower dip speed of 1 mm/min was primarily used to facilitate ethoxy sliane coupling to the quartz surface. However, little difference was observed with this range of dip speeds. Most inner leaflets were allowed to dry for a few hours before the outer leaflet was deposited via the Langmuir−Schaeffer method. In some cases, DSPE-esPEG2k inner leaflets were cured for 40 min at 70 °C before the outer leaflet was deposited. Little difference was observed in the absence of the drying period or curing before deposition the outer leaflet (results not shown).

Bilayers incorporating reactive and nonreactive lipopolymer were also prepared using either DPPC or POPC matrix lipids via the vesicle fusion method. Thin films of dried lipids were dissolved at a concentration of 0.5 mg/mL in ultrapure H_2O and probe tip sonicated to yield small unilamellar vesicles. Vesicle solutions were immediately incubated with a clean quartz substrate for 30 min to allow fusion to take place before flushing with water. Additionally, a hybrid sample preparation technique involving an LB deposited inner leaflet and an outer leaflet deposited via vesicle fusion was investigated. The vesicle fusion and hybrid vesicle fusion techniques were implemented to confirm that the resulting architectures were qualitatively similar to those observed using LB/LS and independent of sample preparation methods.

Neutron and X-ray Reflectivity. Reflectivity, R, is defined as the ratio of the number of particles (neutrons or photons) elastically and specularly scattered from a surface to that of the incident beam. When measured as a function of wave-vector transfer, $Q_Z = |\mathbf{k}_{out} - \mathbf{k}_{in}| = (4\pi \sin \theta)/\lambda$, where θ is the angle of incidence and λ is the wavelength of the beam, the reflectivity curve contains information regarding the sample-normal profile of the in-plane averaged scattering length density (SLD) and is therefore most suited for studies of interfacial, layered films. From the measured reflectivity profile, the thickness, SLD, and roughness of a series of layers normal to the substrate can be determined by minimizing the difference between the measured reflectivity and that obtained from a modeled SLD profile.[14]

Neutron reflectivity (NR) measurements were performed on the SPEAR beamline, a time-of-flight reflectometer, at the Manuel Lujan Jr. Neutron Scattering Center, Los Alamos National Laboratory. Using neutrons wavelengths λ = 2−16 Å and two incident angles, values of the momentum transfer, Q_z, up to 0.25 $Å^{-1}$ and reflectivities down to $R \sim 5 \times 10^{-7}$ were measured. The coherence length of the neutron beam was of order 10 μm and the beam footprint was ~10 × 50 mm. Synchrotron X-ray reflectivity (XR) measurements were carried out at beamline 6-ID at the Advanced Photon Source (Argonne National Laboratory) at a wavelength of λ = 0.545 Å. The high X-ray energy used enabled measurements to be performed at the solid−liquid interface through a 10 mm thick water layer.[15−17]

dx.doi.org/10.1021/la200622e |*Langmuir* 2011, 27, 13618–13628

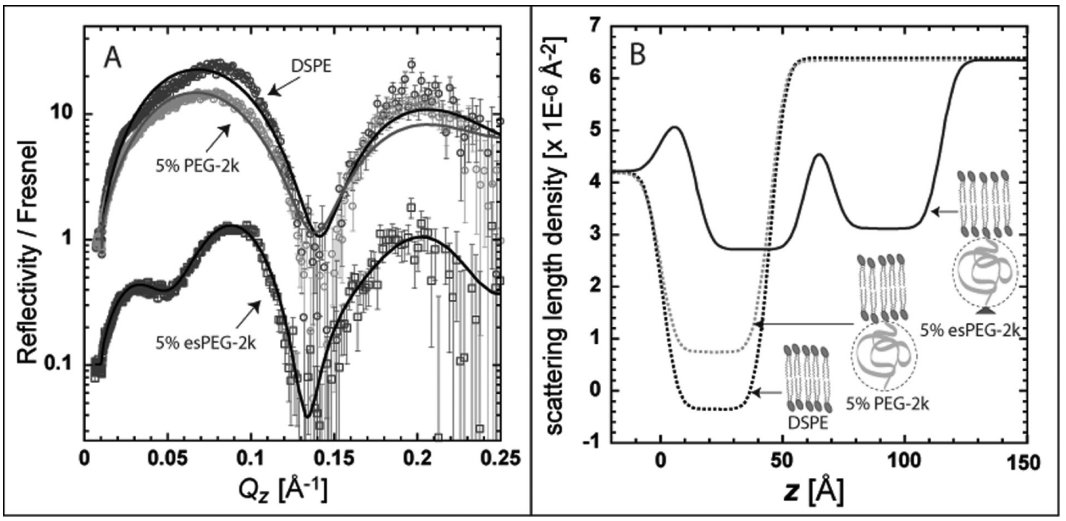

Figure 3. (A) NR divided by Fresnel curve and fits: pure DSPE bilayer (top, dark), untethered 5 mol % DSPE-PEG2k bilayer (top, light), 5 mol % DSPE-esPEG2k tethered cushioned bilayer (bottom, shifted down for clarity). (B) Lines represent box model SLD(z) corresponding to the reflectivities shown: pure DSPE bilayer (dark dashed line), untethered DSPE-PEG2k bilayer (light dashed line), and DSPE-esPEG tethered cushioned bilayer (solid line). The tethered, cushioned bilayer exhibits near complete coverage with approximately half the surface area on top of a thin hydrated layer adjacent to the quartz substrate and the other half supported by ~70 Å of hydrated PEG cushion.

The footprint of the X-ray beam on the sample was $\sim 1 \times 10$ mm^2. High photon flux, relative to the much lower neutron flux, allowed high resolution XR measurements up to $Q_z = 0.8$ Å^{-1}.

NR data was analyzed by minimizing the difference between the measured reflectivity profile and that calculated for a real-space model based on a series of layers describing the polymer cushioned membrane.[18] Using the Parratt formalism, box models described the SLD distribution as a sequence of n constant SLD layers. In this work, the primary contributions to the SLD profile come from hydrogenated lipids and D_2O. At the PEG concentrations studied, the hydrated polymer did not significantly change the SLD of D_2O effectively reducing the system to two components. Error functions were used to connect adjoining layers and describe interfacial roughness. The higher momentum transfer vectors accessible in XR measurements allowed a model-free data fitting approach to be used where the electron density profile normal to the interface was constructed from a series of cubic B-splines.[19] The coefficients in the series of B-splines were determined by constrained nonlinear least-squares methods. We performed over a thousand refinements within the parameter space and present a family of models for each reflectivity data set, all of which satisfy $\chi^2 \leq \chi_{min}^2 + 1$ with typical values of $\chi_{min}^2 < 5$.[17] Highly oscillating profiles, which were not physically reasonable, were excluded. Superimposing the accepted profiles yielded a broad electron density "ribbon" which is a measure of the uncertainty in the real space structure. Box models, consistent with the model-free ribbons, were also used to provide a more quantitative description of the system.

Microscopy and Ellipsometry. Fluorescence microscopy images were taken on a Nikon Eclipse E600 microscope with a 60× magnification water immersion lens. 1,2-Dipalmitoyl-*sn*-glycero-3-phosphoethanolamine-*N*-(7-nitro-2-1,3-benzoxadiazol-4-yl) headgroup labeled fluorescent lipids (NBD-DPPE) were chosen to minimize perturbations to the alkyl chain packing. Samples incorporating 2 mol % NBD-DPPE were prepared by LB/S on quartz substrates and imaged in bulk water at room temperature.

Atomic force microscopy (AFM) was conducted using a Dimension 3100 scanning probe microscope with a Hybrid closed-loop XYZ head and Nanoscope IVa controller (Vecco, Santa Barbara, CA). All samples were deposited on quartz substrates and imaged while submerged in ultrapure water with a direct drive cantilever holder for fluids (Vecco, Santa Barbara, CA). A silicon nitride cantilever with a spring constant of 0.05 N/m was used at a scan rate of 0.5 Hz.

Ellipsometric angles and spatially resolved ellipsometric contrast images were acquired using a commercial Elli2000 imaging system (Nanofilm Technologie, Göttingen, Germany). The ellipsometer employed the polarizer-compensator-sample-analyzer nulling configuration in which a linear polarizer and a quarter-wave plate yield an elliptically polarized incident beam. The polarizer, wave plate, and analyzer positions were then converted to the ellipsometric angles, Δ and Ψ. Using a fluid cell, measurements under aqueous conditions were taken at an incidence angle of 60° and imaged onto a CCD camera through a long-working-distance 10× objective. Silicon substrates with a native oxide were used to enhance the optical contrast with the lipid phase. The specified accuracy in ellipsometric angle determination was 0.01°. Analysis of the measured data with computerized optical modeling led to a deduction of spatially resolved film thickness and complex refractive index values. Using least-squares minimization, the water cushion thickness parameter was varied, and Ψ and Δ values were calculated using the Fresnel equations to match the experimental data.

RESULTS

To investigate the structure of PEG cushioned membranes, measurements of single component DSPE bilayers were compared to bilayers deposited from mixtures of DSPE and lipopolymer (DSPE with PEG polymer covalently bound to the headgroup, Figure 2). The terminus of the PEG chain was either a nonreactive methoxy group (DSPE-PEG) referred to as "nontethered" or a reactive ethoxy silane group (DSPE-esPEG2k) referred to as "tethered". Reactive ethoxy silane groups can form covalent bonds with the quartz substrate and cross-polymerize with each other, which should enhance the stability of the cushioned membrane. Based on previous literature, a 95:5 mol ratio of 2000 MW PEG conjugated DSPE lipids should yield a film where the PEG chains are in the overlapping mushroom regime.[20−22] The thickness of the cushion was therefore expected to be approximately 35 Å; the Flory radius of a PEG-2k chain. Higher and lower

Table 1. Bilayer Neutron Reflectivity Box Model Parameters[a]

	hydrated cushion		supported bilayer (S1)		hydrated cushion		cushioned bilyaer (S2)		D_2O
	Z (Å)	SLD (10^{-6} Å^{-2})	Z (Å)	SLD (10^{-6} Å^{-2})	Z (Å)	SLD (10^{-6} Å^{-2})	Z (Å)	SLD (10^{-6} Å^{-2})	SLD (10^{-6} Å^{-2})
DSPE			45.0 (±1)	−0.33 (±0.15)					6.41 (±0.02)
DSPE-PEG2k, 5 mol %			44.8 (±1)	0.79 (±0.15)					6.38 (±0.02)
DSPE-esPEG, 2 mol %	16.4 (±4)	5.76 (±0.35)	46.9 (±2)	1.53 (±0.1)	10.0 (±3)	5.86 (±0.5)	46.9 (±5)	5.14 (±0.25)	6.23 (±0.03)
DSPE-esPEG, 5 mol %	14.4(±6)	5.28 (±0.45)	45.6 (±3)	2.67 (±0.15)	10.0 (±2)	5.26 (±0.45)	45.6(±3)	3.07 (±0.15)	6.34 (±0.03)
DSPE-esPEG, 6.5 mol %	15.0 (±2)	5.80 (±0.25)	44.0 (±3)	4.31 (±0.15)	13.2 (±2)	3.66 (±0.2)	44.0 (±1)	1.38 (±0.1)	6.31 (±0.02)
DSPE-esPEG, 10 mol %	56.0 (±30)[b]	4.02 (±0.1)[b]	53.6 (±9)[b]	4.30 (±0.05)[b]	22.8 (±9)[b]	4.46 (±0.15)[b]	48.0 (±2)	2.89 (±0.1)	6.07 (±0.02)

[a] Quartz SLD fixed at 4.18×10^{-6} Å^{-2}, and interfacial roughnesses fixed at 5 Å rms. Parameter uncertainties were obtained from a $\chi_{min}^2 = \chi_{min}^2 + 1$ analysis. [b] Model parameters do not correspond to the bimodal cushion description.

concentrations of PEG lipopolymer were also studied to investigate the impact of different PEG grafting densities on the structure and thickness of the cushion. Importantly, previous monolayer studies have observed no phase separation in lipid PEG mixtures at the air−water interface.[22−24]

Neutron Reflectivity. *Pure DSPE.* We start with the reflectivity data and structure of a pure DSPE bilayer deposited on a quartz substrate (Figure 3). Deuterated water (D_2O) was used to maximize the neutron scattering length density (SLD) contrast between the hydrogenated lipids and hydrated regions of the sample. With these contrast conditions, high SLD regions are attributed to water (and hydrated PEG cushion in subsequent studies of lipid and PEG lipopolymer mixtures), while SLD minima correspond to hydrocarbon containing regions of the lipid bilayer. Using the simplest, physically reasonable model, we described the bilayer as a single homogeneous layer of low SLD for the hydrocarbon tails with an additional layer to account for the hydrated cushion. Hydrated lipid headgroups were not explicitly defined but can be approximated by interfacial roughness because they have an SLD intermediate between the lipid tail regions and either the quartz substrate or D_2O superstrate. To further minimize fitting parameters, a 5 Å rms roughness was used at all interfaces which is typical for supported membranes.[17,25]

With this simple model, the structure of a DSPE bilayer was parametrized and fitted yielding a 45.0 Å thickness and a SLD of -0.33×10^{-6} Å^{-2} (Table 1). For comparison, the maximum thickness in angstroms of a saturated hydrocarbon chain can be calculated theoretically using $l_{hc} = 1.5 + 1.265n_c$, where n_c is the number of carbons.[26] Thus, a DSPE bilayer has a theoretical maximum hydrocarbon thickness of 46.0 Å. The fitted thickness matches closely, indicating that the lipid tails are oriented perpendicular to the substrate with little molecular tilt. From the thickness and measured SLD of the hydrocarbon layer, we obtain an average area per molecule of 38.2 Å^2 which is consistent with gel phase PE lipids and indicates the presence of a well packed membrane with near complete surface coverage.[16] This SLD profile for pure DSPE was used as a reference to calculate the membrane coverage for all other systems measured by NR presented in this work.

5 mol % DSPE-PEG2k Bilayers. The neutron reflectivity profile of a supported DSPE bilayer containing 5 mol % untethered DSPE-PEG2k is very similar to that of the pure DSPE bilayer (Figure 3). The minima are in the same positions indicating that the two samples have the same thickness. The shapes of the fitted SLD profiles match, and the nonreactive PEG lipopolymer system's profile shows no evidence of either the lipid region shifting away from the quartz interface due to a PEG cushion or the presence of a second lipid minimum further away from the substrate. The main difference in the SLD profiles is the decreased height of the interference maxima of the DSPE-PEG2k mixture. Decreased interference maxima are due to reduced contrast of the layers, for example, hydrocarbon tails and D_2O, and indicate that this supported bilayer has either partial coverage or is less well ordered than a pure DSPE supported membrane. By assuming the average membrane structure consists of a linear combination of regions of well packed lipids and deuterated water, we calculate an 83% surface coverage for the 5 mol % DSPE-PEG2k mixed membrane. Fluorescent microscopy of the mixed membrane, however, shows a homogeneously fluorescent field indicating that the bare regions are sub-micrometer in size and cannot be resolved optically (Figure 1). The low roughness of the mixed membrane (Table 1) extracted from modeling the reflectivity profile is also consistent with small bare regions below the coherence length of the neutron. The changes in the reflectivity could not be modeled by preserving a high coverage bilayer and introducing a distribution of PEG above or below the bilayer. However, due to the low contrast between hydrated polymer and bulk water, it was not possible to distinguish between two possible architectures: the absence of lipopolymer in a partial coverage bilayer and a partial coverage bilayer with PEG chains extending from the exterior leaflet. Due to this uncertainty, the DSPE-PEG2k system was modeled using a single layer to describe the lipid distribution and the PEG distribution was not explicitly included.

Several sample preparation parameters were adjusted in attempts to construct cushioned membranes including increased mole ratio of PEG conjugated lipids, increased PEG molecular weight, depositing the outer leaflet with and without drying and/or curing, replacing DSPE with a fluid phase matrix lipid, use of an ionic subphase, and employing different contrast conditions. In all of these, cases a lipid membrane was obtained as evidenced by NR measurements; *however, no PEG cushion was detected between the quartz and the supported membrane.* In addition,

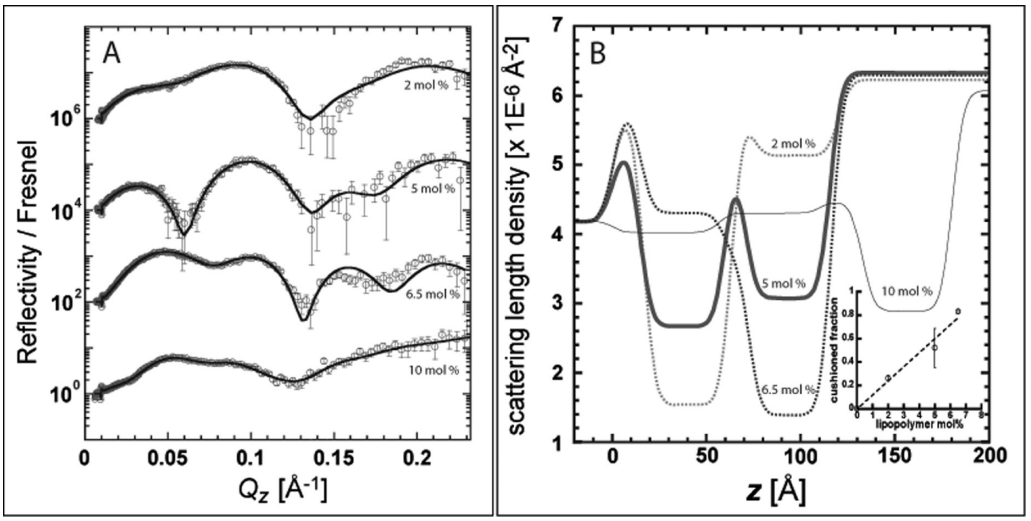

Figure 4. (A) NR divided by Fresnel curve and fits of DSPE-esPEG2k cushioned bilayers with four different molar ratios of lipopolymer. Curves are shifted vertically for clarity by 100. (B) Lines represent box model SLD(z) corresponding to the reflectivities shown. At lower molar ratios (2, 5, 6.5 mol %), there is a bimodal distribution of the bilayer with a greater fraction supported by the polymer cushion as the mole ratio increases. Above a critical point, the bimodal order breaks down and we observe a significant fraction of the membrane cushioned by a thicker and less well-defined mixture of lipid, polymer, and water (10 mol %).

membrane preparation using vesicle fusion was found to yield similar results and did not show evidence of a PEG cushion. We emphasize the results from the more controlled LB/LS deposition method because more complete, less disordered membranes were formed using this approach.

5 mol % DSPE-esPEG2k Bilayers. In contrast to solid supported DSPE and the unreactive DSPE-PEG2k mixed membranes, reflectivity from membranes containing the reactive DSPE-esPEG2k system exhibit multiple minima representing more than one thickness (Figure 3). Two distinct low SLD regions corresponding to the lipid hydrocarbon tails can be seen in the profile: one ∼15 Å away and the other ∼70 Å away from the quartz interface. Both regions are approximately 45 Å thick and represent a bimodal height distribution of the membrane. Based on the SLD profile, roughly half of the membrane is supported by a thin hydrated layer (15 Å) against the substrate and the other half is supported by a much thicker, hydrated PEG cushion (70 Å). Assuming a homogeneous distribution of PEG, a 5 mol % lipopolymer consists of weakly overlapping chains in the mushroom regime with a predicted polymer layer thickness of 38 Å (approximately the Flory radius (R_F)).[21] However, the measured PEG cushion thickness is significantly larger and indicative of an enrichment of lipopolymer in the cushioned regions. The rearrangement and segregation of lipopolmers conserves mass with half the membrane in contact with the underlying substrate and the other, cushioned half, enriched in lipopolymer by a factor of 2. Qualitatively similar structures were measured for the same tethered system using different contrast conditions, prepared after drying and curing, from mixtures with the addition of 5 mol % cholesterol, and from samples where the outer leaflet was deposited via vesicle fusion (data not shown).

Information about the lateral size distribution of the PEG cushioned and noncushioned regions can also be gleaned from the NR measurements. Distinctly different reflectivity profiles would be measured depending on whether the in-plane size of the cushioned regions is larger or smaller than the neutron coherence length (∼10 μm). Beyond the coherence length, the reflectivity signal from the cushioned and noncushioned regions will add incoherently, vis-à-vis a summation of distinct reflectivities from the two different regions. Instead, we observed that the membrane regions scatter coherently, establishing that the cushioned membrane regions are smaller than the ∼10 μm neutron coherence length.

DSPE-esPEG2k Bilayer Concentration Dependence. In addition to 5 mol %, samples containing 2, 6.5, and 10 mol % DSPE-esPEG2k were measured (Figure 4). At lower concentrations of DSPE-esPEG2k, bimodal distributions of the membranes were observed conserving the same separation between the cushioned fraction of the membrane and the substrate. For the 2, 5, and 6.5 mol % mixtures, the cushioned fraction of the membrane was 0.26 ± 0.025, 0.52 ± 0.165, and 0.83 ± 0.02, respectively, showing a linear dependence of the cushioned fraction on the concentration of lipopolymer (inset of Figure 4B). Errors in the membrane's cushioned fraction were estimated by changing the corresponding SLD value while simultaneously allowing all other parameters to adjust until χ^2 was increased by one. This linear trend did not continue at higher concentrations. Instead, at 10 mol % DSPE-esPEG2k, a trimodal distribution of heights was found with a new "cushioned" region detected about 130 Å from the interface. The segregation of cushioned and noncushioned portions of the membrane suggests an equilibrium phase separation occurs. A model detailing this behavior is presented in the Discussion section.

X-ray Reflectivity. To complement the NR measurements, we conducted X-ray reflectivity experiments at the solid liquid interface (Figure 5). Electron density profiles of pure DSPE bilayers on quartz demonstrate the advantages of higher resolution X-ray data. Features that cannot be resolved using NR, such as the low density methyl trough at the bilayer center, become well-defined using X-rays. Consistent with the NR profiles, these measurements show a symmetric DSPE bilayer with near complete coverage that is conformal with the ∼3 Å rms quartz substrate.

XR also reconfirms the finding that the 5 mol % unreactive DSPE-PEG2k systems do not yield cushioned membranes as the

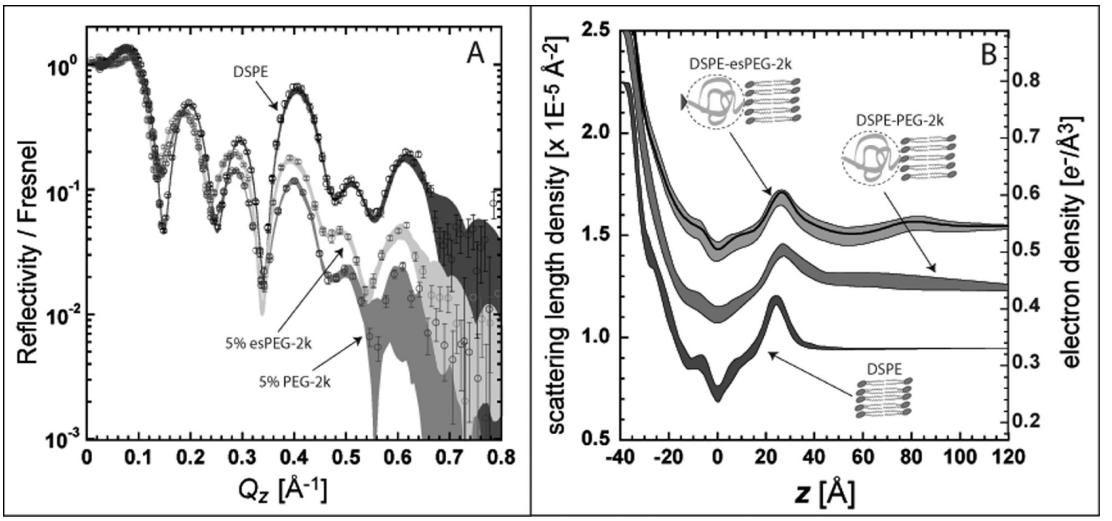

Figure 5. (A) XR divided by Fresnel data and fits: pure DSPE membrane (dark) and a DSPE membrane containing 5 mol % reactive DSPE-esPEG-2k (light). (B) Shaded curves show the family of SLD(z) fits within the selection criteria and $\chi^2 = \chi_{min}^2 + 1$ corresponding to the reflectivities shown: DSPE bilayer (bottom ribbon) and DSPE-esPEG-2k tethered, cushioned membrane (top ribbon). No cushion was observed for nonreactive, untethered PEG systems (middle ribbon). The solid line represents a box model to the DSPE-esPEG data and yields ~10 Å rms roughness for the cushioned bilayer.

bilayers are directly supported by the quartz substrate. Again, low contrast between hydrated polymer and bulk water prevented the determination of lipopolymer concentration in the exterior leaflet of the bilayer. Further, these systems exhibit a high degree of structural variability across a single sample indicating inhomogeneity and disorder in the bilayer but again no evidence of a cushioned membrane. Multiple samples were prepared including ones with a higher mole fraction of DSPE-PEG2k, increased PEG molecular weight, and the addition of cholesterol. For all cases, XR measurements did not detect a cushioned membrane.

XR data from the 5 mol % reactive or tethered DSPE-esPEG2k system is also consistent with neutron measurements. A bimodal distribution of the bilayer was observed with approximately half of the bilayer supported by a thin hydrated layer on the substrate and the other half resting on a thicker hydrated PEG cushion. Due to the lower roughness, the electron density profile of the membrane portion in closer contact with quartz is well-defined and exhibits features similar to those observed for a pure DSPE bilayer. The total electron density profile in this region of the bimodal system is an average of the supported bilayer and the hydrated PEG of the cushioned membrane fraction. As a result, the electron density of the hydrocarbon tail region increased toward that of water while the electron density of the headgroup region was diminished. Electron densities obtained using box models indicate ~50% membrane coverage in contact with the underlying quartz substrate. A bump associated with the outer leaflet headgroups and the decreased electron density corresponding to the tails of the cushioned portion of the bilayer can be seen between 70 and 120 Å from the quartz surface. This is consistent with the membrane resting on a ~70 Å hydrated PEG cushion as found in the NR analysis. Despite the lower visibility compared to the quartz supported portion, box models indicate that approximately half of the membrane is supported by the PEG cushion with a 9 Å rms roughness. Since the primary electron density contrast in lipid bilayers measured in water is the electron rich headgroup and this region is a mere 10 Å thick, the deleterious effects of roughness on the measured structure are more apparent. Conversely, neutron contrast is derived from the 45 Å thick tail regions compared to D_2O, making the quality of that data less susceptible to roughness. Although the XR measurements had superior resolution, the combination of increased roughness and low electron density contrast of the cushioned system did not allow a more precise structural characterization than those based on NR measurements.

Lateral Structure. Both ellipsometry and atomic force microscopy techniques were used to provide complementary information on the lateral structure of tethered PEG cushioned membranes. Ellipsometry measurements yielded an average film thickness of ~60 Å, consistent with the average thickness of the bimodal cushion observed using reflectivity. However, with a lateral resolution of 2 μm, micromapping ellipsometry experiments were unable to resolve the lateral distribution of cushioned regions of the bilayer. Atomic force microscopy was therefore used to provide higher resolution images capable of resolving the lateral structure of reactive PEG cushioned membrane (Figure 6). The distribution of sample heights had a full width at half maximum (fwhm) of ~35 Å and is consistent with the distance between the top surfaces of the solid supported and PEG cushioned bilayers. AFM shows that the cushioned regions of the membrane have sub-micrometer dimensions as indicated by the reflectivity results. The cushioned regions again make up ~50% of the surface area and appear to be distributed fairly uniformly.

DISCUSSION

Cushioned Membrane Structure. The structure of PEG cushioned bilayers was investigated using neutron and X-ray reflectometry as well as complementary techniques to probe in and out-of-plane organization. Previous work has suggested that a hydrated, PEG cushion could be prepared by incorporating unreactive PEG lipopolymers into the supported bilayer.[7,10−13] Here we show that this approach does not yield a cushioned membrane whether vesicle fusion or the more controlled LB/LS deposition method is used. In all cases, there was no increase in

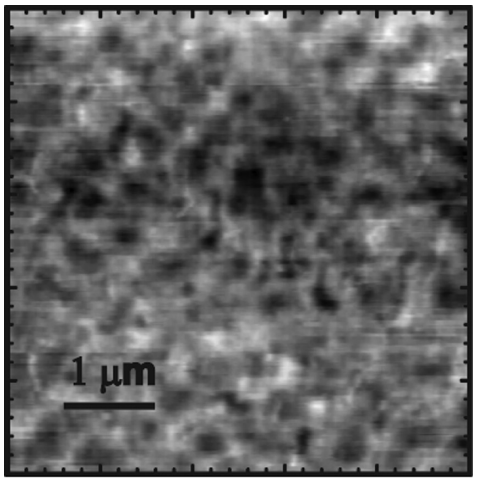

Figure 6. AFM image of a 5 mol % DSPE-esPEG2k tethered, cushioned bilayer. The fwhm of heights was ~35 Å, and lateral structure shows submicrometer domain sizes.

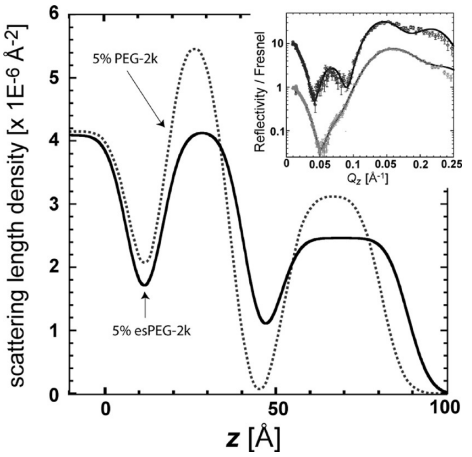

Figure 7. SLD(z) of deuterated lipopolymer monolayers in H_2O vapor. Tethered (dark line) and untethered (dashed line) monolayers composed of DSPE and 5 mol % lipopolymer both exhibit a bimodal distribution of lipids. Inset shows the corresponding NR data and fits.

distance between the membrane and support due to the presence of a PEG cushion and the membrane formed is similar to that found in the absence of the lipopolymer. Indeed, the only difference in structure is that the membrane is more disordered when lipopolymer is incorporated. The absence of a cushion in these systems is also consistent with reported similarities in helical peptide diffusion within bilayers with and without nonreactive lipopolymers on a solid support.[12]

A second, less commonly implemented method to construct cushioned membranes involves incorporating reactive lipopolymers into the membrane to enable covalent tethering of the terminal ends of the polymer to the substrate. A further feature is the potential for enhanced stability through polycondensation of the lipopolymers. This approach was pioneered by Tamm and co-workers as a platform for studying membrane protein diffusion.[4,8] Our structural characterization demonstrates that only portions of the bilayer are supported by hydrated cushioned regions with ~70 Å thicknesses. The remainder of the membrane is separated from the solid support by a thin hydrated layer. This bimodal distribution of the membrane heights maintains conservation of lipopolymer and is consistent with experimental measurements of protein diffusion. For example, lateral mobility of both Cytochrome b_5 and annexin V in tethered lipopolymer supports was found to consist of two populations (referred to as mobile and immobile fractions) with different diffusion coefficients.[8] These observations may have less to do with intrinsic aspects of the proteins' diffusion in a cushioned membrane than with the bimodal distribution of the membrane itself. A similar bimodal membrane distribution for amino terminated PEG-lipids tethered to a COOH functionalized surface has recently been reported.[27] Based on XR measurements, it was suggested that this particular system yielded a mixture of hydrated PEG and lipid micellular disks that cushion the membrane. Despite the higher resolution afforded by XR, the limited electron density contrast makes X-rays a less sensitive probe of the lipopolymer−lipid assemblies than neutrons. Using NR, we observed that in all measurements of the reactive PEG systems the total surface area of both bilayer fractions approximates that of a full coverage membrane. Additionally, AFM measurements (Figure 6) indicate height variations of the

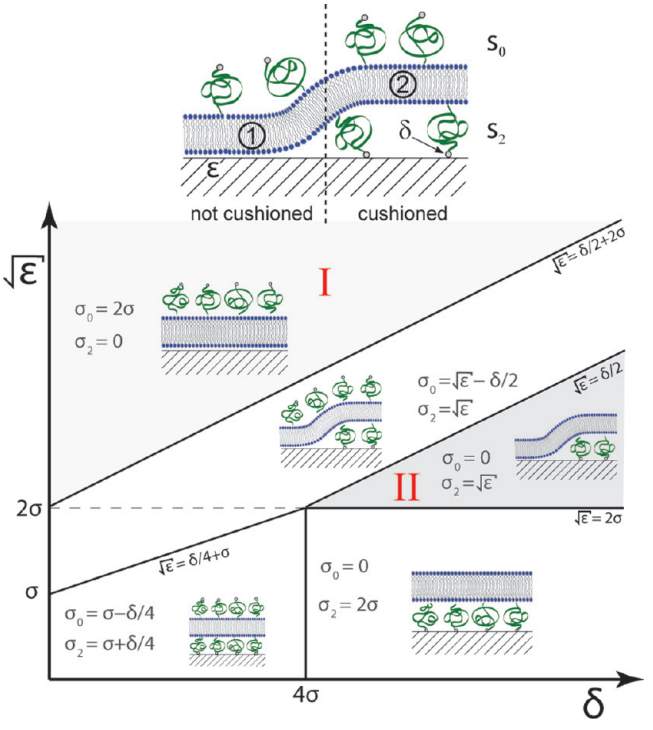

Figure 8. Phase diagram of various cushioned membrane states as a function of the membrane adhesion energy to the substrate, ε, the binding energy of the reactive group to the substrate, δ, and the grafting density of the lipopoymers, σ. For the case of nonreactive lipopolymers $\delta \approx 0$ and $\varepsilon > 0$, the membrane system is in state I. In the reactive lipopolymer case, $\delta > 0$, however, ε is substantial and the membrane system is in state II.

membrane surface commensurate with the bimodal distribution and also demonstrate that the two bilayer populations have sub-micrometer lateral domain sizes. However, these measurements cannot be used to determine the continuity of the bimodally distributed membrane.

To further understand the assembly of lipopolymer bilayers via the more controlled method of LB/LS, we investigated the

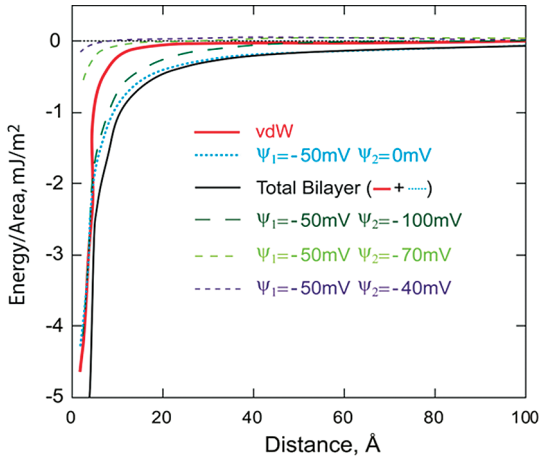

Figure 9. Interaction free energy between a bilayer and quartz as a function of the bilayer surface potential.

structure of just the inner leaflet after the first deposition. Deposited monolayers incorporating PEG lipopolymers were found to exhibit a bimodal distribution of lipids. Neutron reflectivity from both tethered and untethered systems in H_2O vapor are shown in Figure 7. For these studies, lipids with deuterated alkyl tails were used and correspond to high SLD regions while SLD minima correspond to regions containing water and/or hydrated PEG cushion. For both nonreactive and tethered systems, the bimodal distribution reflects regions of the monolayer in contact with the support (uncushioned) and regions on a PEG cushion ~35 Å from the interface. The thickness of the outer distribution of lipids was intermediate between a monolayer and a bilayer. These measurements demonstrate that the monolayer structure is a precursor to the observed structure of the reactive, tethered bilayers and the bimodal distribution is not a consequence of the deposition of the outer leaflet. Since a similar bimodal distribution was not observed for untethered lipopolymer bilayers in bulk water, we hypothesize that in this case the deposition of the outer leaflet enables reorganization of the membrane. Energetic penalties arise from confinement of the lipopolymer between the substrate and the bilayer; hence, in the absence of a reaction to the substrate, it is more favorable for the lipids to rearrange so that lipopolymer is exposed to bulk water. A significant portion of the bilayer may be damaged/removed during this reorganization, explaining the reduced coverage of bilayers containined untethered lipopolymer. When there is only a monolayer, it is unfavorable for the lipopolymers to rearrange.

Lipopolymer Cushion Thermodynamics. The difference in membrane structure between nonreactive or reactive (tethered) lipopolymers can be further explained and quantified using a straightforward thermodynamic analysis of the free energy associated with the various system configurations. We consider two possible states for the phospholipid membrane containing a finite fraction of lipopolymers, as shown in Figure 8A: (1) a surface S_1 of the lipid bilayer is in direct contact with the underlying support, with all lipopolymers in the outer leaflet (uncushioned), and (2) a surface S_2 of the membrane containing lipopolymers in both leaflets, albeit with different surface densities (cushioned). Minimization of the free energy of the whole system with total fixed surface $S = S_1 + S_2$ determines the different surface fractions occupied by each state and the values of their corresponding lipopolymer densities.

The final equilibrium state of this system is controlled by two main parameters: the adhesion energy of the uncushioned membrane with the support, denoted by $\tilde{\varepsilon}$, and the interaction energy with the support of the end-functional group of the lipopolymer, denoted by $\tilde{\delta}$, where $\tilde{\delta} \approx 0$ for the nonreactive lipopolymer and $\tilde{\delta} \gg 0$ for tethered chains. The excluded volume interactions between the polymers depend on the lipopolymer surface density σ: when the surface density is smaller than the overlapping concentration $\sigma \ll \sigma^*$, with $\sigma^* = 1/R_F^2$, chain−chain interactions are negligible. Above σ^*, excluded volume interactions can be accounted for by well-established polymer brush theories. The free energy of this generic system can thus be written as

$$F = S_1\left(k_BTA\left(\frac{\sigma_0}{\sigma^*}\right)^{5/6}\sigma_0 - \tilde{\varepsilon}\right) + S_2\left(k_BTA\left(\frac{\sigma_0}{\sigma^*}\right)^{5/6}\sigma_0 + k_BTA\left(\frac{\sigma_2}{\sigma^*}\right)^{5/6}\sigma_2 - \tilde{\delta}\sigma_2\right) \quad (1)$$

where σ_0 is the polymer density in the outer layer, σ_2 is the polymer density in the inner layer (for uncushioned membranes, $\sigma_2 = 0$), and A is a constant of order unity, $A \approx 1$. Equation 1 can be rewritten as a function of dimensionless quantities by using the following definitions: $x = S_1/S$, $(1 - x) = S_2/S$, $\varepsilon = \tilde{\varepsilon}/(Ak_BT\sigma^*)$, $\delta = \tilde{\delta}/(Ak_BT)$, and by writing all surface densities σ in units of σ^*(i.e., $\sigma_0/\sigma^* = \tilde{\sigma}_0$). For simplicity, the tildes are dropped from the grafting density terms. This yields the free energy per unit surface as

$$\mathcal{T} = \frac{F}{S} = k_BTA\sigma^*\left\{x({\sigma_0}^{11/6} - \varepsilon) + (1-x)({\sigma_0}^{11/6} + {\sigma_2}^{11/6} - \delta\sigma_2)\right\} \quad (2)$$

Conservation of lipopolymer mass between S_1, S_2, and chains that may flip to the external leaflet requires $\sigma_0 x + (1 - x)(\sigma_0 + \sigma_2) = 2\sigma$ or $x = (\sigma_0 + \sigma_2 - 2\sigma)/\sigma_2$. Minimizing $\mathcal{T}$ with respect to σ_0 and σ_2 gives the equilibrium values for these quantities. To make the algebra more tractable, we first approximate the scaling exponent 11/6 by 2 and rescale the free energy per unit area to

$$f = \frac{\mathcal{T}}{k_BTA\sigma^*} = {\sigma_0}^2 + x(-\varepsilon) + (1-x)({\sigma_2}^2 - \delta\sigma_2) \quad (3)$$

With $\partial f/\partial\sigma_0 = \partial f/\partial\sigma_2 = 0$, we find $\sigma_0 = \sqrt{\varepsilon} - \delta/2$, $\sigma_2 = \sqrt{\varepsilon}$, and $f_{min} = (-\delta^2/4) - (2\sqrt{\varepsilon} - \delta)(\sqrt{\varepsilon} - 2\sigma)$. The equilibrium polymer densities are therefore a function of the adhesion energy ε and of the sticking energy δ. However, the set of solutions derived from eq 3, where the two states coexist, only applies in a limited region of the full $\lfloor\delta,\sqrt{\varepsilon}\rfloor$ parameter space, depending on σ, the average polymer density per leaflet. The different possible situations and the corresponding values of σ_0 and σ_2 are summarized in the state diagram shown in Figure 8.

dx.doi.org/10.1021/la200622e |*Langmuir* 2011, 27, 13618–13628

The primary contributions to ε are the van der Waals (VDW) and double-layer electrostatic interaction between the lipid membrane and the quartz support. The VDW energy between the substrate and a bilayer a distance D away can be approximated as:[28]

$$E_{VDW}(D) = -\frac{A_{123}}{12\pi D^2}$$

where the Hamaker constant A_{123} is 7×10^{-21} J.[29] The energy associated with VDW interactions is a significant contribution to the overall attraction of directly supported bilayers (E_{VDW} (5 Å) = -0.75 mJ/m^2) but becomes negligible at the increased bilayer separations (E_{VDW} (65 Å) = -0.004 mJ/m^2) of cushioned geometries.[30] Electric double-layer interactions yield an additional contribution to the energy that can be repulsive or attractive with asymmetric surfaces. To determine the electrostatic contribution for the various scenarios shown in Figure 8, the double layer interactions were calculated by solving the nonlinear Poisson−Boltzmann equation explicitly using a numerical algorithm.[31,32] Given the low dielectric constant of the membrane's hydrocarbon core, we neglect the electrostatic contribution of any PEG-lipids in the outer leaflet of the membrane. Although the electrostatic interaction is always repulsive between the membrane and quartz under conditions of constant surface charge density, when modeled under conditions of constant surface potential, the electrostatic interaction can be large and attractive between surfaces with a significant asymmetry in surface potential. Using a typical surface potential for quartz of $\psi_1 = -50$ mV, the contribution of electrostatic attraction is greatest for the case where the membrane is depleted of lipopolymers ($\psi_2 \rightarrow 0$) as shown in Figure 9.[33] Over a 4−6 pH range, the Debye length varies from 300 to 3000 Å but only modestly impacts the electrostatic interaction for $D < 100$ Å. Assuming a distance cutoff of 5 Å, the maximum electrostatic contribution is $\varepsilon \approx -2$ mJ/m^2 for $\psi_1 = -50$ mV and $\psi_2 = 0$. Anderson and co-workers have recently reported measurements and similar modeling of the interaction of a phosphotidylcholine membrane supported on mica interacting with silica using the surface forces apparatus.[34]

For comparison, we also model the electrostatic interaction for various lipopolymer membrane surface potentials (Figure 9). The surface potential of a membrane containing 5 mol % lipopolymer is negative and can vary from about -40 to -70 mV when the lipopolymer is dispersed in the membrane to -100 mV within higher lipopolymer concentrations cushioned regions.[35−38] Only at small separations ($D < 40$ Å) and very large surface potential differences is the electrostatic contribution for the cushioned system weakly attractive. At separations corresponding to the cushioned regions of the membrane, both the electrostatic interaction and VDW attraction are negligible, $\varepsilon \approx 0$. Thus, when the lipopolymer is nonreactive, $\delta = 0$, it is highly unfavorable for the lipopolymers to remain in the inner leaflet of the membrane, as the "bare" membrane−quartz interaction is more and more attractive as the membrane approaches the quartz surface and ($\psi_2 \rightarrow 0$). Consistent with our experimental measurements, regardless of nonreactive lipopolymer concentration, the system reorganizes into state I of the phase diagram (Figure 8).

In contrast, incorporation of reactive lipopolymers yielded cushioned membranes in state II of the phase diagram. In regions where the membrane is supported on a PEG cushion, $\varepsilon \approx 0$, but the membrane is held to the quartz substrate given a sufficiently high binding energy between the reactive end group and the substrate, $\delta > 0$. Silane coupling agents are known to bond well to quartz through hydrolysis of the ethoxy groups to silanols and subsequent polycondensation of these silanols and surface silanols.[39] With polycondensation of reactive lipopolymers and the energy of a Si−O bond being about 450 kJ/mol or 180 k_BT/bond, it is not surprising that $\delta \gg 0$ and $\sigma_0 = 0$.[39] However, concentrations of reactive lipopolymer $\leq 6.5\%$ always yielded a bimodal system of cushioned and noncushioned regions (state II). Thus, we must also compare the contribution from polymer lateral interactions to ε, where at the minimum $\sigma_2/\sigma^* = \sqrt{\varepsilon}$. We also note that the total PEG concentration was conserved in the inner leaflet. As a result, the cushioned regions in the bimodal system were enriched in PEG and had an average thickness of about $2R_F$ (65 Å). This thickness corresponds to a PEG grafting density of about 1 PEG chain per 450 Å^2, or a concentration of 10 mol % PEG-lipid in the cushioned region.[22] Remarkably, the enriched lipopolymer concentration is in excellent agreement with the value obtained from $\sigma_2/\sigma^* = \sqrt{\varepsilon} \approx 2.7$. This high density $\sigma_2 > \sigma^*$ is also consistent with polycondensation of the lipopolymers which would potentially lead to lateral phase separation of lipopolymer and increase overlap significantly. Further, the local lipopolymer concentration and thickness within cushioned regions was independent of the total lipopolymer concentration of the system. The fraction of membrane supported by the hydrated polymer layer could be controlled, increasing ~0.12 per mol % of lipopolymer incorporated in the mixture. Extrapolating from this linear relationship, a homogenously cushioned membrane would be expected for mixtures containing 8.5 mol % of 2k MW PEG lipopolymer.

A further comment on the 65 Å thickness of the cushioned region is that it is only marginally larger than the uncushioned bilayer thickness. Thus, the bimodal distribution may also be partially stabilized from portions of the cushioned bilayer sitting atop the bilayer in contact with the underlying quartz substrate. Some support for this scenario comes from the structure of the membrane system at higher lipopolymer concentration. At 10 mol %, a trimodal distribution was observed with the outermost membrane region located ~130 Å from the substrate (Figure 4). This separation is only slightly less than a fully stretched PEG2k chain (158 Å) and would require an unphysically large lateral enrichment of lipopolymer. However, such a separation could result from continuation of a bilayer stacking mechanism to a third layer. If the equilibrium cushion structure relies on overlapping membrane portions or bilayer stacking, this may be a factor inhibiting the formation of complete homogeneous cushions.

CONCLUSION

In this work, NR and XR were used to structurally characterize supported lipid bilayers containing PEG lipopolymer. While the reactive PEG system studied here did not yield homogenously cushioned membranes, these results demonstrate a method for creating full coverage membranes supported by laterally segregated, sub-micrometer cushions. When the lipopolymer is functionalized with a reactive end group, bimodally distributed cushion architectures are obtained. Without a strong binding interaction, the lipopolymer is excluded from the inner leaflet of the membrane and a hydrated cushion was not obtained. Such platforms may prove useful for investigating the function of individual membrane proteins within isolated

membrane microdomains. A thermodynamic description and accompanying phase diagram for lipopolymer membrane cushions show that these systems are highly tunable and can yield qualitatively different cushion architectures. For example, these systems can be manipulated into different regions within the phase diagram by changing surface charge density, altering the support material to modulate VDW interactions, or using reactive groups with different binding energies. Finally, other factors not captured by the thermodynamic description presented here may contribute to the equilibrium membrane cushion structure. For instance, cross-polymerization of the polymer tethering moieties may result in lateral phase separation of cushioned membrane regions and bilayer stacking may also play a role in the final structure.

■ ACKNOWLEDGMENT

This work was supported by NSF Chemistry Division through Grant CHE-0957868. Preliminary measurements were supported by NSF DMR-0606564. Neutron measurements were performed at the SPEAR reflectometer at the Los Alamos Neutron Scattering Center (LANSCE). LANSCE is supported by DOE Contract W7405-ENG-36 and the Advanced Photon Source by DOE Contract W-31-109-Eng-38. We thank Doug Robinson for beamline assistance on beamline 6-ID at the Advanced Photon Source. We also thank Adrian Brozell for assistance with AFM measurements.

■ REFERENCES

(1) Castellana, E. T.; Cremer, P. S. Solid supported lipid bilayers: From biophysical studies to sensor design. *Surf. Sci. Rep.* **2006**, *61*, 429–444.

(2) Sackmann, E.; Tanaka, M. Supported membranes on soft polymer cushions: fabrication, characterization and applications. *Trends Biotechnol.* **2000**, *18*, 58–64.

(3) Tanaka, M.; Sackmann, E. Polymer-supported membranes as models of the cell surface. *Nature* **2005**, *437*, 656–663.

(4) Kiessling, V.; Tamm, L. K. Measuring distances in supported bilayers by fluorescence interference-contrast microscopy: Polymer supports and SNARE proteins. *Biophys. J.* **2003**, *84*, 408–418.

(5) Majewski, J.; Wong, J. Y.; Park, C. K.; Seitz, M.; Israelachvili, J. N.; Smith, G. S. Structural studies of polymer-cushioned lipid bilayers. *Biophys. J.* **1998**, *75*, 2363–2367.

(6) Naumann, C. A.; Frank, C. W.; Prucker, O.; Lehmann, T.; Rühe, J.; Knoll, W. Lateral mobility of phospholipids in tethered polymer-supported membranes. *Biophys. J.* **2000**, *78*, 273a–273a.

(7) Naumann, C. A.; Prucker, O.; Lehmann, T.; Rühe, J.; Knoll, W.; Frank, C. W. The polymer-supported phospholipid bilayer: Tethering as a new approach to substrate-membrane stabilization. *Biomacromolecules* **2002**, *3*, 27–35.

(8) Wagner, M. L.; Tamm, L. K. Tethered polymer-supported planar lipid bilayers for reconstitution of integral membrane proteins: Silane-polyethyleneglycol-lipid as a cushion and covalent linker. *Biophys. J.* **2000**, *79*, 1400–1414.

(9) Smith, H. L.; Jablin, M. S.; Vidyasagar, A.; Saiz, J.; Watkins, E.; Toomey, R.; Hurd, A. J.; Majewski, J. Model Lipid Membranes on a Tunable Polymer Cushion. *Phys. Rev. Lett.* **2009**, *102*, 238101.

(10) Albertorio, F.; Diaz, A. J.; Yang, T.; Chapa, V. A.; Kataoka, S.; Castellana, E. T.; Cremer, P. S. Fluid and air-stable lipopolymer membranes for biosensor applications. *Langmuir* **2005**, *21*, 7476–7482.

(11) Diaz, A. J.; Albertorio, F.; Daniel, S.; Cremer, P. S. Double cushions preserve transmembrane protein mobility in supported bilayer systems. *Langmuir* **2008**, *24*, 6820–6826.

(12) Merzlyakov, M.; Li, E.; Gitsov, I.; Hristova, K. Surface-supported bilayers with transmembrane proteins: Role of the polymer cushion revisited. *Langmuir* **2006**, *22*, 10145–10151.

(13) Rossi, C.; Homand, J.; Bauche, C.; Hamdi, H.; Ladant, D.; Chopineau, J. Differential mechanisms for calcium-dependent protein/membrane association as evidenced from SPR-binding studies on supported biomimetic membranes. *Biochemistry* **2003**, *42*, 15273–15283.

(14) Kjaer, K. Some Simple Ideas on X-Ray Reflection and Grazing-Incidence Diffraction from Thin Surfactant Films. *Phys. B* **1994**, *198*, 100–109.

(15) Miller, C. E.; Majewski, J.; Kuhl, T. L. Characterization of single biological membranes at the solid-liquid interface by X-ray reflectivity. *Colloids Surf., A* **2006**, *284*, 434–439.

(16) Miller, C. E.; Majewski, J.; Watkins, E. B.; Kuhl, T. L. Part I: An x-ray scattering study of cholera toxin penetration and induced phase transformations in lipid membranes. *Biophys. J.* **2008**, *95*, 629–640.

(17) Watkins, E. B.; Miller, C. E.; Mulder, D. J.; Kuhl, T. L.; Majewski, J. Structure and Orientational Texture of Self-Organizing Lipid Bilayers. *Phys. Rev. Lett.* **2009**, *102*, 228102.

(18) Parratt, L. G. Surface Studies of Solids by Total Reflection of X-Rays. *Phys. Rev.* **1954**, *95*, 359–369.

(19) Pedersen, J. S.; Hamley, I. W. Analysis of Neutron and X-Ray Reflectivity Data by Constrained Least-Squares Methods. *Phys. B* **1994**, *198*, 16–23.

(20) Baekmark, T. R.; Elender, G.; Lasic, D. D.; Sackmann, E. Conformational Transitions of Mixed Monolayers of Phospholipids and Poly(Ethylene Oxide) Lipopolymers and Interaction Forces with Solid-Surfaces. *Langmuir* **1995**, *11*, 3975–3987.

(21) Kenworthy, A. K.; Hristova, K.; Needham, D.; McIntosh, T. J. Range and Magnitude of the Steric Pressure between Bilayers Containing Phospholipids with Covalently Attached Poly(Ethylene Glycol). *Biophys. J.* **1995**, *68*, 1921–1936.

(22) Kuhl, T. L.; Leckband, D. E.; Lasic, D. D.; Israelachvili, J. N. Modulation of Interaction Forces between Bilayers Exposing Short-Chained Ethylene-Oxide Headgroups. *Biophys. J.* **1994**, *66*, 1479–1488.

(23) Kuhl, T. L.; Majewski, J.; Howes, P. B.; Kjaer, K.; von Nahmen, A.; Lee, K. Y. C.; Ocko, B.; Israelachvili, J. N.; Smith, G. S. Packing stress relaxation in polymer-lipid monolayers at the air-water interface: An X-ray grazing-incidence diffraction and reflectivity study. *J. Am. Chem. Soc.* **1999**, *121*, 7682–7688.

(24) Majewski, J.; Kuhl, T. L.; Gerstenberg, M. C.; Israelachvili, J. N.; Smith, G. S. Structure of phospholipid monolayers containing poly(ethylene glycol) lipids at the air-water interface. *J. Phys. Chem. B* **1997**, *101*, 3122–3129.

(25) Charitat, T.; Bellet-Amalric, E.; Fragneto, G.; Graner, F. Adsorbed and free lipid bilayers at the solid-liquid interface. *Eur. Phys. J. B* **1999**, *8*, 583–593.

(26) Tanford, C. Micelle Shape and Size. *J. Phys. Chem.* **1972**, *76*, 3020.

(27) Daniel, C.; Sohn, K. E.; Mates, T. E.; Kramer, E. J.; Rädler, J. O.; Sackmann, E.; Nickel, B.; Andruzzi, L. Structural characterization of an elevated lipid bilayer obtained by stepwise functionalization of a self-assembled alkenyl silane film. *Biointerphases* **2007**, *2*, 109–118.

(28) Israelachvili, J. N. *Intermolecular and Surface Forces*, 2nd ed.; Academic Press: London, 1992.

(29) Marra, J.; Israelachvili, J. Direct Measurements of Forces between Phosphatidylcholine and Phosphatidylethanolamine Bilayers in Aqueous-Electrolyte Solutions. *Biochemistry* **1985**, *24*, 4608–4618.

(30) The distances used for the VDW calculations are the NR model separations between the substrate and hydrocarbon regions less 10 Å to account for the lipid head groups.

(31) Grabbe, A.; Horn, R. G. Double-Layer and Hydration Forces Measured between Silica Sheets Subjected to Various Surface Treatments. *J. Colloid Interface Sci.* **1993**, *157*, 375–383.

(32) Developed by Grabbe, the algorithm explicitly computes the electrostatic potential between two flat surfaces using a relaxation method on a finite mesh.

(33) Ducker, W. A.; Senden, T. J.; Pashley, R. M. Measurement of Forces in Liquids Using a Force Microscope. *Langmuir* **1992**, *8*, 1831–1836.

(34) Anderson, T. H.; Min, Y.; Weirich, K. L.; Zeng, H.; Fygenson, D.; Israelachvili, J. N. Formation of Supported Bilayers on Silica Substrates. *Langmuir* **2009**, *25*, 6997–7005.

(35) Kuhl, T. L.; Leckband, D. E.; Lasic, D. D.; Israelachvili, J. N. Modulation of Interaction Forces Between Bilayers Exposing Short-Chained Ethylene Oxide Headgroups. *Biophys. J.* **1994**, *66*, 1479–1487.

(36) Moore, N. W.; Kuhl, T. L. The role of flexible tethers in multiple ligand-receptor bond formation between curved surfaces. *Biophys. J.* **2006**, *91*, 1675–1687.

(37) Sheth, S. R.; Leckband, D. Measurements of attractive forces between proteins and end-grafted poly(ethylene glycol) chains. *Proc. Natl. Acad. Sci. U.S.A.* **1997**, *94*, 8399–404.

(38) Wong, J. Y.; et al. Direct measurement of a tethered ligand-receptor interaction potential. *Science* **1997**, *275*, 820–822.

(39) Wen, K.; et al. Postassembly chemical modification of a highly ordered organosilane multilayer: New insights into the structure, bonding, and dynamics of self-assembling silane monolayers. *ACS Nano* **2008**, *2*, 579–599.